Naked mole rats can undergo developmental, oncogene-induced and DNA damage-induced cellular senescence

Yang Zhao[a,1], Alexander Tyshkovskiy[b,c,1], Daniel Muñoz-Espín[d,e], Xiao Tian[a], Manuel Serrano[d,f,g], Joao Pedro de Magalhaes[h], Eviatar Nevo[i,2], Vadim N. Gladyshev[c], Andrei Seluanov[a,2], and Vera Gorbunova[a,2]

[a]Department of Biology, University of Rochester, Rochester, NY 14627; [b]Center for Data-Intensive Biomedicine and Biotechnology, Skolkovo Institute of Science and Technology, 143028 Moscow, Russia; [c]Division of Genetics, Department of Medicine, Brigham and Women's Hospital, Harvard Medical School, Boston, MA 02115; [d]Tumor Suppression Group, Spanish National Cancer Research Centre, 28029 Madrid, Spain; [e]Cancer Research UK Cambridge Centre Early Detection Programme, Department of Oncology, University of Cambridge, Hutchison/MRC Research Centre, Cambridge CB2 0XZ, United Kingdom; [f]Institute for Research in Biomedicine, Barcelona Institute of Science and Technology, 08028 Barcelona, Spain; [g]Catalan Institute of Advanced Studies, 08010 Barcelona, Spain; [h]Integrative Genomics of Ageing Group, Institute of Ageing and Chronic Disease, University of Liverpool, Liverpool L7 8TX, United Kingdom; and [i]Institute of Evolution, University of Haifa, 3498838 Haifa, Israel

Contributed by Eviatar Nevo, December 28, 2017 (sent for review December 14, 2017; reviewed by Vadim Fraifeld and Stephen L. Helfand)

Cellular senescence is an important anticancer mechanism that restricts proliferation of damaged or premalignant cells. Cellular senescence also plays an important role in tissue remodeling during development. However, there is a trade-off associated with cellular senescence as senescent cells contribute to aging pathologies. The naked mole rat (NMR) (*Heterocephalus glaber*) is the longest-lived rodent that is resistant to a variety of age-related diseases. Remarkably, NMRs do not show aging phenotypes until very late stages of their lives. Here, we tested whether NMR cells undergo cellular senescence. We report that the NMR displays developmentally programmed cellular senescence in multiple tissues, including nail bed, skin dermis, hair follicle, and nasopharyngeal cavity. NMR cells also underwent cellular senescence when transfected with oncogenic Ras. In addition, cellular senescence was detected in NMR embryonic and skin fibroblasts subjected to γ-irradiation (IR). However, NMR cells required a higher dose of IR for induction of cellular senescence, and NMR fibroblasts were resistant to IR-induced apoptosis. Gene expression analyses of senescence-related changes demonstrated that, similar to mice, NMR cells up-regulated senescence-associated secretory phenotype genes but displayed more profound down-regulation of DNA metabolism, transcription, and translation than mouse cells. We conclude that the NMR displays the same types of cellular senescence found in a short-lived rodent.

senescence | naked mole rat | aging

Cellular senescence (CS) is a state of permanent cell-cycle arrest that cells adopt in response to stress. Multiple stresses induce CS, including telomere shortening that occurs during replicative senescence, DNA damage such as γ-irradiation leading to stress-induced premature senescence (SIPS), and oncogene-induced senescence (OIS). In addition, programmed CS occurs during embryonic development, playing a critical role in tissue remodeling (1, 2).

CS is believed to be an important mechanism to prevent cancer (3, 4). However, CS also has its deleterious effects. Accumulation of senescent cells impairs tissue function and promotes aging. Persistent senescent cells also display senescence-associated secretory phenotype (SASP), which may result in aging-related diseases, including cancer (5–7). Remarkably, elimination of senescent cells extends the health and life span of mice (8, 9), indicating that CS contributes to aging and age-related diseases (10, 11).

The naked mole rat (NMR) (*Heterocephalus glaber*) is the longest-lived rodent with a maximum life span of over 30 y (12). Remarkably, NMRs are extremely cancer resistant and do not show aging phenotypes or age-related diseases until very late in their lives (13). Several mechanisms have been identified that contribute to longevity and cancer resistance of the NMR. Our earlier studies revealed that cultured NMR fibroblasts exhibit early contact inhibition (ECI) (14), which contributes to its cancer resistance. ECI could be abrogated by the removal of high-molecular-mass hyaluronan (15). Furthermore, an additional product from the INK4a/b locus, the p15/p16 hybrid, has a stronger ability to induce cell-cycle arrest than either p15 or p16, contributing to the cancer resistance of the NMR (16). Naked-mole-rat–induced pluripotent stem cells are inefficient in forming teratomas (17, 18), and NMR cells have a much higher translation fidelity than mouse cells (19). NMRs display better protein stability and less age-associated increase in cysteine oxidation during aging (20). Furthermore, NMRs have markedly higher levels of cytoprotective NRF2-signaling activity (21). We previously showed that, similarly to other small rodents, naked mole rats do not display replicative senescence and express telomerase in somatic tissues (22–24). However, other types of senescence have not been investigated.

Significance

The naked mole rat (NMR) is the longest-lived rodent with a maximum life span of over 30 years. Furthermore, NMRs are resistant to a variety of age-related diseases and remain fit and active until very advanced ages. The process of cellular senescence has evolved as an anticancer mechanism; however, it also contributes to aging and age-related pathologies. Here, we characterize cellular senescence in the NMR. We find that naked mole rat cells undergo three major types of cellular senescence: developmental, oncogene-induced, and DNA damage-induced. Senescent NMR cells displayed many common features with senescent mouse cells, including activation of a senescence-associated secretory phenotype. These results demonstrate that the NMR retains the major types of cellular senescence responses despite its exceptional longevity.

Author contributions: Y.Z., A.T., D.M.-E., M.S., J.P.d.M., E.N., V.N.G., A.S., and V.G. designed research; Y.Z., A.T., D.M.-E., M.S., V.N.G., A.S., and V.G. performed research; X.T. and J.P.d.M. contributed new reagents/analytic tools; Y.Z., A.T., D.M.-E., M.S., J.P.d.M., E.N., V.N.G., A.S., and V.G. analyzed data; and Y.Z., A.T., D.M.-E., M.S., E.N., V.N.G., A.S., and V.G. wrote the paper.

Reviewers: V.F., Ben-Gurion University of the Negev; and S.L.H., Brown University.

The authors declare no conflict of interest.

[1]Y.Z. and A.T. contributed equally to this work.

[2]To whom correspondence may be addressed. Email: vera.gorbunova@rochester.edu, nevo@research.haifa.ac.il, or andrei.seluanov@rochester.edu.

This article contains supporting information online at www.pnas.org/lookup/suppl/doi:10.1073/pnas.1721160115/-/DCSupplemental.

Since CS contributes to aging and age-related disease, from which NMRs are remarkably protected, we set out to investigate CS in the NMR. We found that NMR cells undergo developmentally programmed senescence, OIS, and SIPS. However, induction of SIPS in the NMR required a higher dose of DNA damage compared with the mouse, and NMR cells were remarkably protected from DNA-damage–induced apoptosis. Transcriptome analysis of senescent NMR cells showed similar up-regulation of SASP genes, but more robust down-regulation of DNA replication, transcription, and translation pathways compared with senescent mouse cells. We conclude that NMRs retain all of the major types of cellular senescence response; however, NMR senescent cells display certain unique features that may contribute to cancer resistance and longevity.

Results

Naked Mole Rats Display Developmental Senescence. Stress-induced senescence is believed to have originated from developmentally programmed senescence (1). Programmed senescence plays an important role in tissue remodeling during development. To determine whether NMR cells undergo developmental senescence, senescence-associated β-galactosidase (SA-β-gal) staining was performed on several tissues of newborn NMRs and mice. Whole-mount SA-β-gal staining of newborn NMRs showed positive staining in the nails and in focal areas of the skin (Fig. 1*A*). Histological sections showed SA-β-gal–positive cells in the nail bed (Fig. 1*B*), in the skin dermis, and in the dermis surrounding the hair follicles (Fig. 1*C*) of newborn NMRs. These locations did not show SA-β-gal–positive staining in newborn mice. The implication that the SA-β-gal–positive areas are senescent was also supported by the fact that they were positive for p21. In addition, senescence has been recently reported to be a physiological mechanism that controls the rate of bone growth (25). In this regard, NMRs and mice had positive SA-β-gal staining in the bone marrow (vertebra and skull; *SI Appendix*, Fig. S1). SA-β-gal–positive cells were negative for the proliferation marker Ki67 (*SI Appendix*, Fig. S1). These results suggest that NMR cells undergo programmed senescence during development and that senescence occurs in several locations unique to the NMR, as well as in other locations that are common with mice. Senescent cells present in the hair follicles of the newborn NMRs may be the reason behind NMR hairlessness.

Naked Mole Rat Fibroblasts Undergo Oncogene-Induced Senescence. To investigate whether NMR fibroblasts undergo oncogene-induced senescence, embryonic and skin primary fibroblasts from mice (MEF and MSF, respectively) and NMRs (NEF and NSF, respectively), derived from three animals of each species, were transfected with either GFP or HRasV12 expression plasmids. Cells were maintained for 12 d and then subjected to SA-β-gal staining and BrdU incorporation assays. Cells of both species displayed a senescent morphology (Fig. 2*A*), SA-β-gal staining (Fig. 2*B*), and reduction in DNA synthesis (Fig. 2*C*), indicating that NMR cells undergo oncogene-induced senescence.

Attenuated SIPS and Apoptosis in NMR Fibroblasts in Response to γ-Irradiation. γ-Irradiation induces SIPS in human and mouse fibroblasts by activating a DNA damage response (26). To examine whether SIPS can be induced in the NMR, its embryonic and skin fibroblasts as well as mouse embryonic and skin fibroblasts derived from three animals of each species were subjected to 10 or 20 Gy of γ-irradiation. Senescence was quantified by SA-β-gal staining and BrdU incorporation. All four cell types showed SA-β-gal–positive staining in response to γ-irradiation. Notably, at 10 Gy of γ-irradiation NMR showed fewer SA-β-gal–positive cells than mouse cells. At the higher 20-Gy dose both mice and NMR displayed similar numbers of SA-β-gal–positive cells (Fig. 3 *A* and *B*). Consistent with the SA-β-gal staining result, at 10 Gy NMR cells did not show a significant drop in BrdU incorporation, while in mouse cells BrdU incorporation dropped significantly. In the NMR cells, a significant drop in BrdU incorporation occurred only at 20 Gy (Fig. 3*C*). Taken together, these results suggest that NMR cells are more resistant to induction of SIPS than mouse cells and require a higher dose to achieve the same percentage of senescent cells.

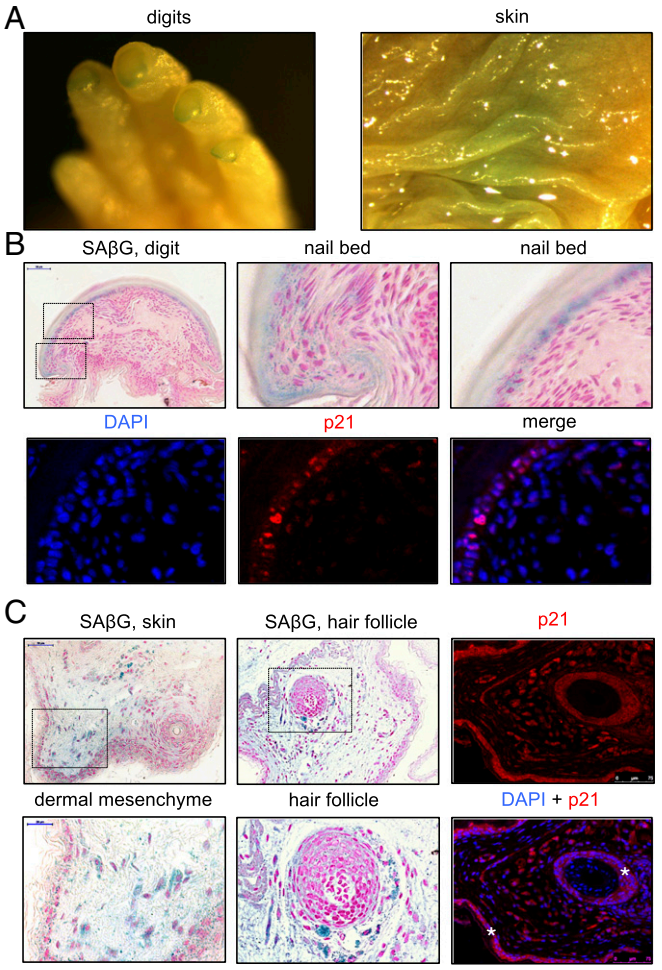

Fig. 1. Developmental CS in the nail bed, dermis, and hair follicles of newborn NMR. (*A*) Examples of SA-β-gal-positive structures in newborn NMR after whole-mount staining. (*B*) Whole-mount SA-β-gal staining of newborn NMR digits. Panels show sections of newborn NMR digits counterstained with nuclear fast red. Magnified views of the nail bed area are indicated by dashed squares. DAPI (blue) and p21 (red) immunofluorescence of digit sections is shown, as indicated. (*C*) Whole-mount SA-β-gal staining of newborn NMR skin. Panels show sections of the newborn NMR skin counterstained with nuclear fast red. Magnified views of the dermal mesenchyme and hair follicle are indicated by dashed squares. DAPI (blue) and p21 (red) immunofluorescence of skin sections is also shown. Note that the p21 signal in dermal cells is nuclear. In contrast, the red immunofluorescence signal in the skin epidermis and in the hair-follicle outer root sheath is mostly cytoplasmic (indicated with asterisks), and, therefore, it is most likely a nonspecific signal.

Cell-cycle arrest and SIPS are triggered by the induction of p21 cyclin-dependent kinase inhibitor. Strong p21 induction occurred in MEF and NEF cells, but the p21 response was lower in the NSF cells compared with the NEF and MSF cells (Fig. 3 *D* and *E*).

In addition to senescence, cells may undergo DNA-damage–induced apoptosis, particularly when the DNA damage is severe (27). Both MEF and MSF cells underwent massive apoptosis in a dose-dependent manner while NEF and NSF cells showed only a slight increase in apoptosis after 20 Gy irradiation, and no significant

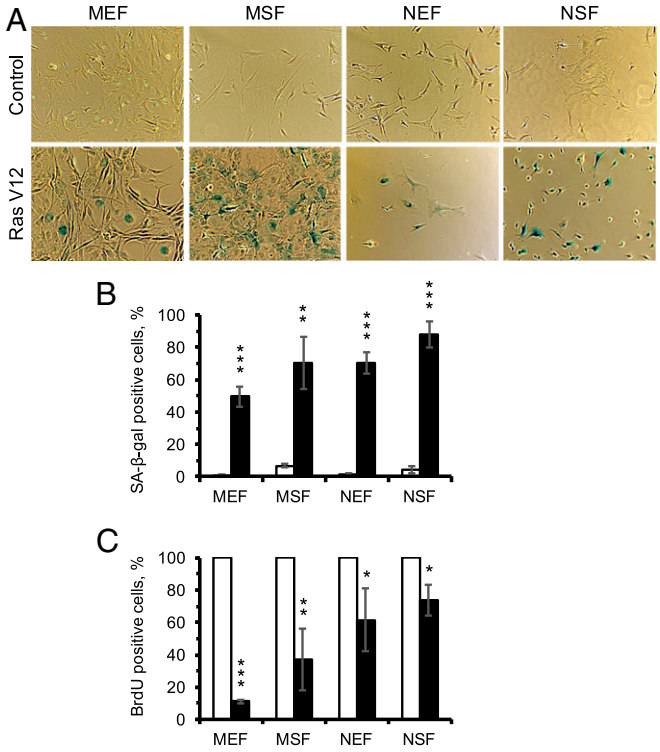

Fig. 2. Oncogene-induced CS of mouse and NMR fibroblasts. (*A*) Images of SA-β-gal staining of mouse and NMR embryonic and skin fibroblasts 12 d after transfection with HRasV12. (*B*) Quantification of β-gal–positive cells of mouse and NMR fibroblasts in response to HRasV12. (*C*) BrdU incorporation in mouse and NMR fibroblasts 12 d after transfection with HRasV12. MEF, mouse embryonic fibroblasts; MSF, mouse skin fibroblasts; NEF, NMR embryonic fibroblasts; NSF, NMR skin fibroblasts. The results are mean ± SD (n = 3). $^{**}P < 0.01$, $^{***}P < 0.001$.

apoptosis was observed under 10 Gy irradiation (Fig. 3*F*), suggesting that NMR cells are resistant to γ-irradiation (IR)-induced apoptosis.

To examine if the NMR and mouse fibroblasts experienced the same physical DNA damage in response to γ-irradiation, we subjected cells to 10 and 20 Gy of γ-irradiation and collected immediately for comet assay. All four types of cells had similarly increased tail DNA in response to γ-irradiation (Fig. 3*G* and *SI Appendix*, Fig. S2), suggesting that NMR and mouse cells sustain similar levels of DNA damage. Taken together, these results show that NMR fibroblasts undergo SIPS in response to γ-irradiation, but senescence and apoptotic responses are attenuated.

Comparison of Gene Expression Changes in Response to γ-Irradiation in NMR and Mouse Fibroblasts. To perform an unbiased characterization of the differences in response to γ-irradiation between NMR and the mouse at the gene expression level, we subjected MEF, MSF, NEF, and NSF cells to 20 Gy of γ-irradiation and performed RNA sequencing (RNAseq). Total RNA was collected from both treated and untreated cells 12 d later, a time point when all irradiated cells displayed positive SA-β-gal staining (Fig. 3*A*), and sequenced. Three biological replicates (primary cells isolated from three different animals) were sequenced for each condition.

To achieve uniform annotation of sequenced genes between the species, we mapped the reads to the set of mouse and NMR orthologs, which, after filtering and normalization, resulted in the coverage of 10,959 genes. Following this procedure, samples across species and cell types showed similar gene expression profile distribution, making them appropriate for subsequent analysis (*SI Appendix*, Fig. S3). To assess the gene expression patterns across cell types and species, we performed principal component analysis (*SI Appendix*, Fig. S4). The samples segregated more predominantly by species (first component; 51.5% variance explained) than by the type of fibroblasts (mainly second component; 24.7% variance explained; *SI Appendix*, Fig. S4). As expected, irradiated samples also tended to cluster with their paired controls, confirmed by Pearson correlation matrix of gene expression profiles (*SI Appendix*, Figs. S4 and S5). Interestingly, gene expression across different NMR samples was

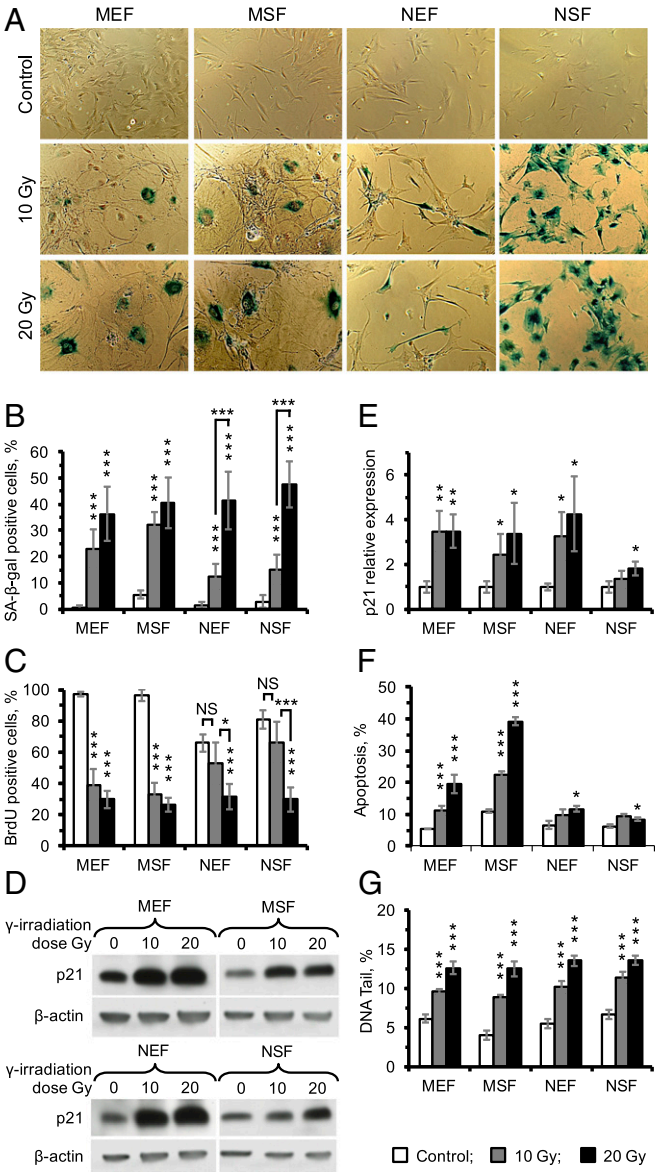

Fig. 3. The γ-irradiation–induced CS of mouse and NMR fibroblasts. (*A*) Images of SA-β-gal staining of mouse and NMR embryonic and skin fibroblasts in response to 10 or 20 Gy of IR. (*B*) Quantification of β-gal–positive cells of mouse and NMR fibroblasts in response to IR. (*C*) BrdU incorporation in mouse and NMR fibroblasts 2 d after IR. (*D*) Expression of p21 in response to IR. Samples were harvested 2 d after IR and tested using Western blot. (*E*) Quantification of p21 expression. (*F*) Apoptosis of mouse and NMR fibroblasts in response to IR. Three days after IR, cells were harvested and subjected to an Annexin V apoptosis assay using FACS. (*G*) Comet assay quantifying DNA damage in mouse and NMR fibroblasts induced by IR. MEF, mouse embryonic fibroblasts; MSF, mouse skin fibroblasts; NEF, NMR embryonic fibroblasts; NSF, NMR skin fibroblasts. For all except *G*, results are mean ± SD (n = 5); for comet assay (*G*), results are mean ± SEM (n = 100). $^{*}P < 0.05$, $^{**}P < 0.01$, $^{***}P < 0.001$.

CELL BIOLOGY

more tight than across mouse samples (*SI Appendix*, Fig. S4), possibly reflecting chromosomal instability typical of cultured mouse cells (28). To compare within-species and within-cell-type variation of gene expression changes in response to γ-irradiation, we calculated gene fold changes averaged across replicates for each species and cell type and built a Pearson correlation matrix of the four analyzed groups. The correlation matrix showed clear separation by species, confirming that within-species variation is lower than variation in the within-cell types (*SI Appendix*, Fig. S6).

To identify changes induced by γ-irradiation in the NMR and mouse transcriptomes, we examined differentially expressed genes for each species and cell type using edgeR (29). We used a Benjamini–Hochberg procedure to adjust for multiple comparisons and qualified as significantly changed the genes with the adjusted $P < 0.05$ and fold change of >2 in any direction. Approximately two times more differentially expressed genes were detected in mouse fibroblasts (651 for MEF and 751 for MSF) compared with NMR fibroblasts (323 for NEF and 220 for NSF) (Fig. 4*A*). Notably, the number of statistically significant up-regulated genes exceeded the number of down-regulated genes for all analyzed groups (Fig. 4*A*). In addition, many up-regulated genes were shared across cell types and species (*SI Appendix*, Fig. S7). Although we observed within-species clustering of gene fold changes, we also observed statistically significant positive Pearson correlation of genes logFC between any two analyzed groups (Pearson correlation test $P < 2{\cdot}2^{-16}$ for all comparisons), even when comparing different cell types of NMR and mice ($\rho = 0.17$ for mice EF vs. NMR SF and $\rho = 0.2$ for mice SF vs. NMR EF) (*SI Appendix*, Fig. S6), pointing to the existence of a general gene expression response of fibroblasts to γ-irradiation across species and types of fibroblasts.

To further investigate the transcriptome response of NMR and mice fibroblasts to γ-irradiation, we performed Gene Set Enrichment Analysis (GSEA) for each of the four analyzed groups using the GO Biological Process (GO BP) and Molecular Function and the Kyoto Encyclopedia of Genes and Genomes (KEGG) and REACTOME database gene sets as a reference. Interestingly, although more genes were identified as differentially expressed in mouse fibroblasts, more pathways were detected as enriched in NMRs (1,151 for NEF and 551 for NSF) than in mice (140 for MEF and 262 for MSF) (Fig. 4*A*), indicating that gene expression changes in the NMR are less drastic, but more systematic and nonstochastic. Indeed, SDs of logFC induced by γ-irradiation in mouse samples are statistically significantly higher than those in NMR samples ($P = 0.015$), as determined by Mann–Whitney *U* test (*SI Appendix*, Fig. S8), pointing to higher stochasticity and scale of transcriptome changes in mice. Accordingly, more enriched functions in the NMR were preserved when we examined each gene set source individually using GSEA (*SI Appendix*, Fig. S9).

Many enriched functions and pathways were shared across cell types and species. They include up-regulation of genes involved in the immune response and down-regulation of genes involved in cell cycle, DNA replication, translation, and ribosome protein genes (Fig. 4*B*). When we analyzed the number of enriched functions (with a GSEA adjusted $P < 0.05$) shared by embryonic and skin fibroblasts within each species, we discovered more functions perturbed in NMR fibroblasts (213 up-regulated and 257 down-regulated) than in mouse cells (61 up-regulated and 42 down-regulated), consistent with the results for every individual cell type (*SI Appendix*, Fig. S10). This finding confirms the observation that the NMR response to γ-irradiation includes regulation of many common biological processes with mice, but in NMRs these changes are more systematic and organized. A complete list of functions that changed in both types of fibroblasts in each species, grouped by functional groups, is shown in Dataset S1.

Enriched gene sets shared by mice and NMRs also included SASP genes (as characterized in refs. 5–7), consistently activated in analyzed groups (GSEA $P < 10^{-3}$ for MSF, NEF, and NSF), except MEF samples (GSEA $P = 0.26$) (Fig. 4*B*). Correlation and linear model analyses showed consistency between expression of SASP genes in the NMR and mouse (*SI Appendix*, Fig. S11) with the Pearson correlation coefficient equal to 0.53 ($P = 2.8{\cdot}10^{-5}$) for SF and 0.63 for EF ($P = 2.9{\cdot}10^{-7}$).

In addition to common functions, we discovered many enriched pathways specific for certain species. Naked mole rat cells displayed unique down-regulation of transcription, spliceosome, and mitochondrial translation, which may indicate a more profound inhibition of cellular metabolism. On the other hand, pathways involved in protein and glycoprotein metabolism, lipid metabolism, lysosome, extracellular matrix, and oxidative stress response were uniquely activated in the NMR (Fig. 4*B*). In addition, apoptotic processes were activated in the mouse (GSEA adjusted $P = 9{\cdot}10^{-3}$ for MEF and 10^{-3} for MSF), but not in the NMR (GSEA adjusted $P = 0.125$ for NEF and 0.302 for NSF) cells after γ-irradiation, which is consistent with the elevated levels of apoptosis that we observed in the mouse cells (Fig. 3*F*). A complete list of functions significantly activated or inhibited in at least one of the analyzed groups can be found in Dataset S2.

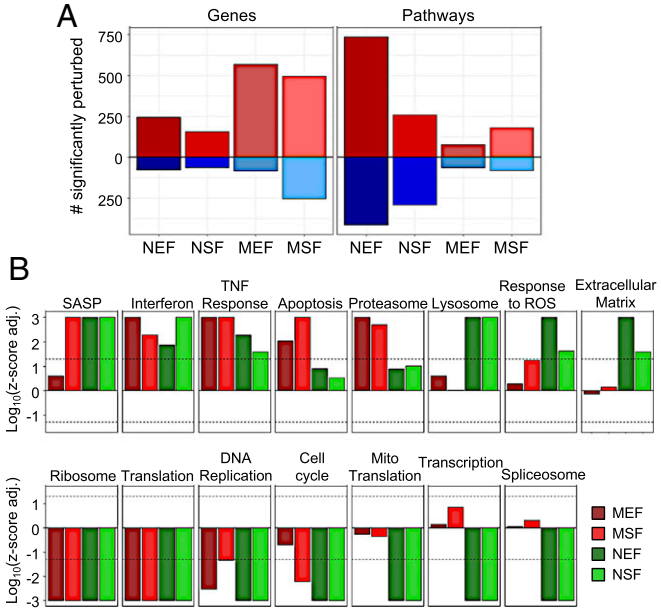

Fig. 4. Functional enrichment of changes induced by γ-irradiation in NMR and mouse fibroblasts. (*A*) Numbers of identified statistically significant differentially expressed genes (Benjamini–Hochberg adjusted $P < 0.05$; fold change > 2 in any direction) and enriched functions (q-value < 0.05) in NMR and mouse fibroblasts in response to γ-irradiation. Up- and down-regulated entities are shown in red and blue, respectively. Although both mouse fibroblast types show more changes at the level of individual genes, these changes are less systematic at the functional level compared with the NMR cells. (*B*) Pathway enrichment of genes differentially induced by γ-irradiation based on GSEA. *Z*-scores (in logarithmic scale) corresponding to presented functions are shown for each analyzed group. *Z*-scores of mouse and NMR fibroblasts are colored in red and green, respectively. Dashed line corresponds to the q-value of 0.05. Pathways include: Apoptosis (REACTOME); Cell cycle (KEGG); Interferon, IFN alpha/beta signaling (REACTOME); Lysosome (KEGG); Mito Translation, mitochondrial translation (GO BP); Proteasome (KEGG); Ribosome (KEGG); SASP, senescence-associated secretory phenotype genes; Spliceosome, (KEGG); TNF response, response to tumor necrosis factor (GO BP); Transcription (REACTOME).

To obtain further insights into similarities and differences in the transcriptome response to γ-irradiation in mice and NMRs, we examined genes with the most similar and distinct expression changes across these species. With the Benjamini–Hochberg adjusted P value threshold equal to 0.05 and the fold change threshold equal to 2, we detected 224 genes with common changes and 782 genes with distinct changes between the NMR and mouse (*SI Appendix*, Fig. S12*A*). Interestingly, the majority of genes with distinct behavior were genes up-regulated in the mouse but not in the NMR. These genes included apoptotic genes (GSEA adjusted $P = 0.045$), consistent with individual GSEA results (*SI Appendix*, Fig. S12*B*). Among them, we could identify the transcription factor *E2f1*, which mediates p53-dependent and -independent apoptosis, together with its positive regulator *Tfdp1*, apoptosis activators *Cflasr*, *Dapk1*, and *Pmaip1* (*Noxa*), with the latter known to be associated with radiation response, cell-surface death receptor *Fas*, several cytoskeleton-related genes (*Plec*, *Lmnb1*, *Dsp*), as well as several genes related to proteasome structure and activity (*Psmb3*, *Psmc4*, *Psmd6*, *Psme4*). Other enriched pathways associated with genes activated in mice compared with NMR include transcription (GSEA adjusted $P = 3.87{\cdot}10^{-3}$) and spliceosome (GSEA adjusted $P = 8.2{\cdot}10^{-3}$). On the other hand, genes associated with ribosome (GSEA adjusted $P = 3.28{\cdot}10^{-3}$) and lysosome (GSEA adjusted $P = 3.28{\cdot}10^{-3}$) show significantly stronger inhibition in mice compared with the NMR (*SI Appendix*, Fig. S12).

GSEA performed on the list of commonly changed genes showed that pathways such as TNF signaling (GSEA adjusted $P < 3.53{\cdot}10^{-5}$), ribosome (GSEA adjusted $P < 1.43{\cdot}10^{-5}$), and cell cycle (GSEA adjusted $P < 1.43{\cdot}10^{-5}$) together with SASP genes are commonly changed not only at the level of functional enrichment, but also at the level of the same individual genes involved in these pathways (*SI Appendix*, Fig. S12). The complete list of significant functions (with adjusted $P < 0.05$) for common and distinct genes can be found in Dataset S3.

Together, these results indicate that NMR and mice share many common gene expression signatures in response to γ-irradiation, both at the level of individual genes and at the level of enriched pathways. They include DNA replication, transcription, translation, cell cycle, and immune response. At the same time, some biological processes, such as apoptosis, glycoprotein metabolism, lysosome, extracellular matrix, and oxidative stress response, show distinct behavior in these species, pointing to unique adaptations of NMR fibroblasts to DNA damage. Generally, although mouse fibroblasts demonstrate more substantial transcriptome remodeling at the level of individual genes, NMR fibroblasts show more organized and systematic regulation of gene pathways upon entry to CS, thus hinting of higher robustness and control of their gene expression profile.

Discussion

CS plays important roles in developmental tissue remodeling (1) and tumor suppression in response to DNA damage (30, 31). We previously showed that NMRs, similarly to mice and other small-bodied rodents, do not display replicative senescence and continuously express telomerase (23, 24). Here, we demonstrate that NMR cells undergo developmentally programmed senescence, as well as oncogene- and IR-induced senescence (Fig. 5). These results show that despite their exceptional longevity and resistance to age-related diseases, NMRs still possess all major types of CS programs. Developmental senescence may be an evolutionarily conserved process not directly impacting the aging process. However, senescent cells accumulating in adult organisms have been linked to multiple age-related pathologies including cancer (30), atherosclerosis (32), and osteoarthritis (33). Elimination of senescent cells in mice displaying premature aging due to genomic instability increases animal life span, and elimination of senescent cells in wild-type mice increases their health span (8, 9). However, our results indicate that the naked mole rat did not achieve longevity by eliminating the process of CS. Remarkably, senescent NMR cells exhibit a typical signature of SASP response including the conserved SASP factor CXCL-1 (GRO-α), which is believed to promote the growth of pre-malignant epithelial cells (6). Thus, the SASP response, which is linked to the proinflammatory and disease-promoting effects of senescence is also preserved in the NMR.

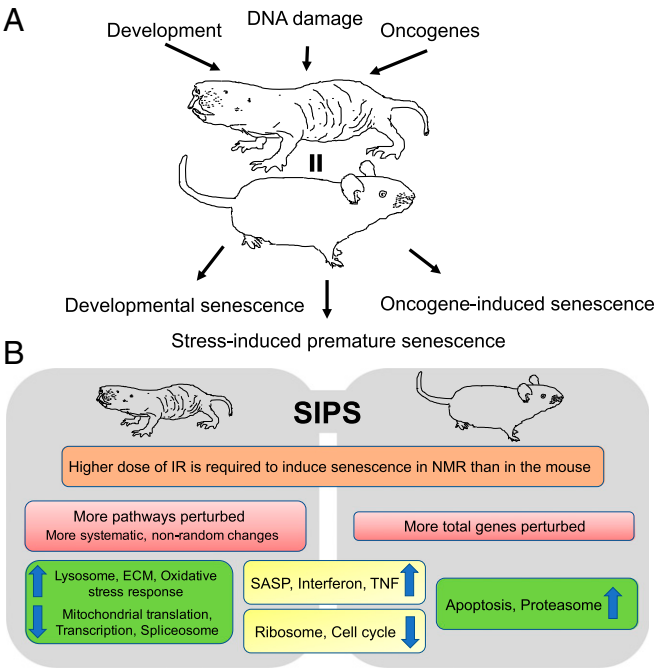

Fig. 5. CS in the naked mole rat. (*A*) Naked mole rat cells, similar to mouse cells, can undergo the three major types of CS. (*B*) Summary of common and distinct features of IR-induced SIPS between the NMR and the mouse.

NMRs may be somewhat protected from the induction of SIPS due to their higher resistance to the damaging agents. We observed that at 10 Gy of IR NMR cells displayed markedly fewer senescent cells then at 20 Gy, while mouse cells displayed a high level of senescent cells at both IR doses. Thus, NMRs may accumulate fewer SIPS senescent cells during aging. This could be partly a result of better repair mechanisms or the protective role from the high-molecular-mass hyaluronan (HA) secreted by NMR cells (15). Ultimately, it would be interesting to quantify senescent cells in aged NMRs. This would shed light on whether senescent cells accumulate in vivo at similar rates to the shorter-lived species. This experiment, however, is logistically challenging as aged, 20- to 30-y-old NMRs are not readily available.

Furthermore, NMR fibroblasts were resistant to IR-induced apoptosis. Our RNAseq data demonstrated clearly that, unlike the mouse fibroblasts, in the NMR p53 and apoptosis signaling pathways were not induced by IR. Therefore, we hypothesize that the resistance of NMR cells to IR-induced apoptosis may be due to the blunted induction of p53 signaling. Reaching confluence and cell-cycle extension have been shown to promote resistance to apoptosis by allowing additional time to repair damage (27, 34). The NMR fibroblasts have a very slow rate of cell proliferation in culture, with early contact inhibition associated with the induction of $p16^{INK4a}$ and the additional INK4a/b hybrid product $pALT^{INK4a/b}$ (14, 16). The $pALT^{INK4a/b}$ hybrid product induces stronger cell-cycle arrest in response to UV and IR (16). The strong cell-cycle arrest in NMR cells likely plays important roles in resistance to apoptosis. Generally, the resistance to IR-induced apoptosis in NMR may reflect its higher threshold for stress tolerance due to better DNA repair mechanisms or the protective effects of HA.

Since the naked mole rat is extremely cancer-resistant and long-lived, a question that could be raised is whether the resistance to apoptosis provides any benefit for cancer resistance or longevity. In terms of eliminating preneoplastic cells, apoptosis seems to have stronger ability to prevent tumorigenesis (27). However, too much apoptosis may deplete stem-cell reserves and contribute to frailty in old age (35, 36).

Gene expression analysis of NMR cells made senescent by IR exposure (Fig. 5*B*) showed that many gene expression changes upon CS were conserved with mice such as induction of SASP, IFN, TNF response, and inhibition of protein translation and the cell cycle. The changes unique to NMR included induction of lysosomal genes, oxidative stress response, changes in extracellular matrix, and inhibition of transcription, spliceosome, and mitochondrial translation. These unique changes may have a cytoprotective effect. Induction of lysosomal genes suggests activation of autophagy. Autophagy plays important roles in response to DNA damage (37–40). Previous study has shown that NMR has higher autophagy (41). Here, we show that NMR fibroblasts are likely to undergo autophagy and induction of oxidative stress response upon exposure to IR, possibly contributing to NMR resistance to stresses. Furthermore, inhibition of transcription and mitochondrial translation, observed only in the NMR, suggests that senescent NMR cells inhibit metabolic activities, thereby reducing pathogenesis of senescent cells. It has been observed that down-regulation of the mTOR pathway in senescent cells ameliorates the senescent phenotype (42, 43).

Interestingly, fewer genes were changed in the senescent NMR cells, compared with mouse cells, but these genes organized in markedly more functional pathways. This result suggests that the senescence-related gene expression changes in the NMR are more systematic and nonrandom. Taken together, these unique features of NMR senescent cells may reduce the pathogenic properties of senescent cells and contribute to NMR longevity.

In summary, we have demonstrated that NMR cells undergo developmental, oncogene-induced and stress-induced senescence. This result shows that evolution of a long life span does not eliminate the CS response. On the contrary, NMR cells were more resistant to apoptosis than mouse cells, suggesting that NMR cells favor senescence to apoptotic response. While the SASP phenotype was conserved in the NMR cells, these cells displayed a unique transcriptional signature that may reduce the pathogenic effects of senescent cells and contribute to naked mole rat longevity and cancer resistance.

Materials and Methods

All animal experiments were approved by and performed in accordance with guidelines set up by the University of Rochester Committee on Animal Resources. Detailed experimental procedures including analysis of senescence by SA-β-Gal staining, cell culture, overexpression of an oncogene, Western blotting, BrdU-incorporation assay, comet assay, flow cytometry, and RNA-seq analysis are provided in *SI Appendix, SI Materials and Methods*.

ACKNOWLEDGMENTS. This research was supported by National Institute of Aging grants (to V.N.G., A.S., and V.G.) and by the Life Extension Foundation (A.S. and V.G.).

1. Muñoz-Espín D, et al. (2013) Programmed cell senescence during mammalian embryonic development. *Cell* 155:1104–1118.
2. Storer M, et al. (2013) Senescence is a developmental mechanism that contributes to embryonic growth and patterning. *Cell* 155:1119–1130.
3. Collado M, et al. (2005) Tumour biology: Senescence in premalignant tumours. *Nature* 436:642.
4. Xue W, et al. (2007) Senescence and tumour clearance is triggered by p53 restoration in murine liver carcinomas. *Nature* 445:656–660.
5. Coppé JP, et al. (2008) Senescence-associated secretory phenotypes reveal cell-nonautonomous functions of oncogenic RAS and the p53 tumor suppressor. *PLoS Biol* 6: 2853–2868.
6. Coppé JP, et al. (2010) A human-like senescence-associated secretory phenotype is conserved in mouse cells dependent on physiological oxygen. *PLoS One* 5:e9188.
7. Coppé JP, Desprez PY, Krtolica A, Campisi J (2010) The senescence-associated secretory phenotype: The dark side of tumor suppression. *Annu Rev Pathol* 5:99–118.
8. Baker DJ, et al. (2016) Naturally occurring p16(Ink4a)-positive cells shorten healthy lifespan. *Nature* 530:184–189.
9. Baar MP, et al. (2017) Targeted apoptosis of senescent cells restores tissue homeostasis in response to chemotoxicity and aging. *Cell* 169:132–147.e16.
10. Yanai H, Fraifeld VE (2017) The role of cellular senescence in aging through the prism of Koch-like criteria. *Ageing Res Rev* 41:18–33.
11. Tacutu R, Budovsky A, Yanai H, Fraifeld VE (2011) Molecular links between cellular senescence, longevity and age-related diseases–A systems biology perspective. *Aging (Albany NY)* 3:1178–1191.
12. Edrey YH, Hanes M, Pinto M, Mele J, Buffenstein R (2011) Successful aging and sustained good health in the naked mole rat: A long-lived mammalian model for biogerontology and biomedical research. *ILAR J* 52:41–53.
13. Buffenstein R (2008) Negligible senescence in the longest living rodent, the naked mole-rat: Insights from a successfully aging species. *J Comp Physiol B* 178:439–445.
14. Seluanov A, et al. (2009) Hypersensitivity to contact inhibition provides a clue to cancer resistance of naked mole-rat. *Proc Natl Acad Sci USA* 106:19352–19357.
15. Tian X, et al. (2013) High-molecular-mass hyaluronan mediates the cancer resistance of the naked mole rat. *Nature* 499:346–349.
16. Tian X, et al. (2015) INK4 locus of the tumor-resistant rodent, the naked mole rat, expresses a functional p15/p16 hybrid isoform. *Proc Natl Acad Sci USA* 112:1053–1058.
17. Miyawaki S, et al. (2016) Tumour resistance in induced pluripotent stem cells derived from naked mole-rats. *Nat Commun* 7:11471.
18. Tan L, et al. (2017) Naked mole rat cells have a stable epigenome that resists iPSC reprogramming. *Stem Cell Rep* 9:1721–1734.
19. Azpurua J, et al. (2013) Naked mole-rat has increased translational fidelity compared with the mouse, as well as a unique 28S ribosomal RNA cleavage. *Proc Natl Acad Sci USA* 110:17350–17355.
20. Pérez VI, et al. (2009) Protein stability and resistance to oxidative stress are determinants of longevity in the longest-living rodent, the naked mole-rat. *Proc Natl Acad Sci USA* 106:3059–3064.
21. Lewis KN, et al. (2015) Regulation of Nrf2 signaling and longevity in naturally long-lived rodents. *Proc Natl Acad Sci USA* 112:3722–3727.
22. Kim EB, et al. (2011) Genome sequencing reveals insights into physiology and longevity of the naked mole rat. *Nature* 479:223–227.
23. Seluanov A, et al. (2007) Telomerase activity coevolves with body mass not lifespan. *Aging Cell* 6:45–52.
24. Seluanov A, et al. (2008) Distinct tumor suppressor mechanisms evolve in rodent species that differ in size and lifespan. *Aging Cell* 7:813–823.
25. Li C, et al. (2017) Programmed cell senescence in skeleton during late puberty. *Nat Commun* 8:1312.
26. d'Adda di Fagagna F (2008) Living on a break: Cellular senescence as a DNA-damage response. *Nat Rev Cancer* 8:512–522.
27. Childs BG, Baker DJ, Kirkland JL, Campisi J, van Deursen JM (2014) Senescence and apoptosis: Dueling or complementary cell fates? *EMBO Rep* 15:1139–1153.
28. Gaztelumendi N, Nogués C (2014) Chromosome instability in mouse embryonic stem cells. *Sci Rep* 4:5324.
29. Robinson MD, McCarthy DJ, Smyth GK (2010) edgeR: A Bioconductor package for differential expression analysis of digital gene expression data. *Bioinformatics* 26:139–140.
30. Campisi J (2005) Senescent cells, tumor suppression, and organismal aging: Good citizens, bad neighbors. *Cell* 120:513–522.
31. Qian Y, Chen X (2010) Tumor suppression by p53: Making cells senescent. *Histol Histopathol* 25:515–526.
32. Childs BG, et al. (2016) Senescent intimal foam cells are deleterious at all stages of atherosclerosis. *Science* 354:472–477.
33. Jeon OH, et al. (2017) Local clearance of senescent cells attenuates the development of post-traumatic osteoarthritis and creates a pro-regenerative environment. *Nat Med* 23:775–781.
34. Rochette PJ, Brash DE (2008) Progressive apoptosis resistance prior to senescence and control by the anti-apoptotic protein BCL-xL. *Mech Ageing Dev* 129:207–214.
35. Tyner SD, et al. (2002) p53 mutant mice that display early ageing-associated phenotypes. *Nature* 415:45–53.
36. Gatza C, Moore L, Dumble M, Donehower LA (2007) Tumor suppressor dosage regulates stem cell dynamics during aging. *Cell Cycle* 6:52–55.
37. Czarny P, Pawlowska E, Bialkowska-Warzecha J, Kaarniranta K, Blasiak J (2015) Autophagy in DNA damage response. *Int J Mol Sci* 16:2641–2662.
38. Wang Y, et al. (2016) Autophagy regulates chromatin ubiquitination in DNA damage response through elimination of SQSTM1/p62. *Mol Cell* 63:34–48.
39. Kalamida D, Karagounis IV, Giatromanolaki A, Koukourakis MI (2014) Important role of autophagy in endothelial cell response to ionizing radiation. *PLoS One* 9:e102408.
40. Ito H, Daido S, Kanzawa T, Kondo S, Kondo Y (2005) Radiation-induced autophagy is associated with LC3 and its inhibition sensitizes malignant glioma cells. *Int J Oncol* 26: 1401–1410.
41. Zhao S, et al. (2014) High autophagy in the naked mole rat may play a significant role in maintaining good health. *Cell Physiol Biochem* 33:321–332.
42. Laberge RM, et al. (2015) MTOR regulates the pro-tumorigenic senescence-associated secretory phenotype by promoting IL1A translation. *Nat Cell Biol* 17:1049–1061.
43. Leontieva OV, Demidenko ZN, Blagosklonny MV (2014) Contact inhibition and high cell density deactivate the mammalian target of rapamycin pathway, thus suppressing the senescence program. *Proc Natl Acad Sci USA* 111:8832–8837.